Available online at www.sciencedirect.com
SCIENCE DIRECT®
Polymer 44 (2003) 3679–3685
polymer
www.elsevier.com/locate/polymer

Transport properties of organic vapors in nanocomposites of organophilic layered silicate and syndiotactic polypropylene

Giuliana Gorrasi[a], Mariarosaria Tortora[a], Vittoria Vittoria[a,*], Dirk Kaempfer[b], Rolf Mülhaupt[b]

[a]*Dipartimento di Ingegneria Chimica e Alimentare, Università di Salerno, Via Ponte Don Melillo, 84084 Fisciano (SA), Italy*
[b]*Freiburger Materialforschungszentrum und Institut für Makromolekulare Chemie der Albert-Ludwigs Universität, Stefan-Meier-Str. 31, D-79104 Freiburg i.Br., Germany*

Received 5 November 2002; received in revised form 10 March 2003; accepted 27 March 2003

Abstract

Syndiotactic polypropylene (sPP) nanocomposites were obtained by melt blending synthetic fluorohectorite modified octadecyl ammmonium ions (OLS), and maleic-anhydride-grafted isotactic polypropylene (iPP-g-MA) as compatibilizer. The composition of the inorganic material was varied between 5 and 20 w/w%. Films of the composites were obtained by hot press molding the pellets. Melt-direct polymer intercalation of sPP into the OLS gave rise to nanocomposites in which the silicate layers were delaminated at low clay contents, and ordered to intercalated structures at the highest clay content. The elastic modulus was higher than for the pure polymer in a wide temperature range and increased with the inorganic content. The transport properties were measured for dichloromethane and *n*-pentane. The sorption was reduced compared to pure sPP. There were not significative differences between the samples having different inorganic contents. The diffusion coefficient decreased with increasing clay content. Permeability (*P*) showed a strong decreasing dependence on the clay content. The improvement of the barrier properties was largely caused by the reduced diffusion.

Keywords: Nanocomposites; Sorption; Diffusion

1. Introduction

Layered silicate/polymer composites are hybrid inorganic–organic materials, in which the matrix and the reinforcing material are truly dispersed on nanoscale [1–4]. Because of their nanometer size features, nanocomposites possess unique properties typically not shared by the conventional microcomposites and are interesting from a technological point of view. The most common nanocomposites are composed of polymers and organically modified montmorillonite. The physical dimensions of these disc-like shaped silicate layers of the unmodified clay are approximately 100 nm in diameter, and 1 nm in thickness. Staking of the silicate layers leads to a regular van der Waals gap between the layers, which was termed as the interlayer gallery. Isomorphic substitution within the layers generates negative charges that are normally counterbalanced by cations like Na^+, Ca^{2+}, or K^+ residing in the gallery space [2,4–5]. Ion exchange reactions with various organic cations, such as alkylammonium cations, expand the interlayer space and make the silicate hydrophobic. The organic cations promote the miscibility of the silicate layers with the polymer matrix. In most cases, the synthesis of nanocomposites involves either intercalation of a suitable monomer followed by polymerization and then exfoliation of the layered host into their nanoscale elements, or by melt intercalation directly into the polymer using a conventional extrusion process [6–12]. This method is the most versatile and environmentally benign approach. Nanocomposites based on polyolefins are of a very high interest because they are the polymers with the highest consumption, due to their low cost and wide versatility in terms of properties and applications. Several papers on isotactic polypropylene (iPP) nanocomposites have been published [13–15]. Nanocomposite formation is a very attractive route to enhance the matrix stiffness of rather flexible syndiotactic polypropylene (sPP) [16]. When functionalized iPP was added as compatibilizer, the formation of core/shell type

* Corresponding author.
E-mail address: vvittoria@unisa.it (V. Vittoria).

0032-3861/03/$ - see front matter © 2003 Elsevier Science Ltd. All rights reserved.
doi:10.1016/S0032-3861(03)00284-2

nanoparticles were observed with silicate platelets embedded in a thin shell of the functionalized iPP.

sPP, recently obtained with high tacticity and high molecular weight using new metallocene catalysts [17–18], is receiving great attention owing to its particular properties [19–28] and a very complex polymorphic behavior not yet fully clarified [29–41]. From an industrial point of view the mechanical properties are not as good as for the isotactic polypropylene but this makes the preparation of sPP-layered silicate nanocomposites even more attractive in terms of improving the competitiveness of the sPP.

As in the case of iPP, problems occur due to absence of polar groups in the backbone of the polymer and the resulting incompatibility with the silicate layers even when they are modified with long chain alkylammonium ions [42–44]. The commonly used method to prepare sPP-layered silicate nanocomposites is to use functionalised oligomers as compatibilizers such as iPP or sPP, respectively, grafted with maleic anhydride onto the backbone. The driving force for the intercalation may be originated from the hydrogen bonding between the pendant succinic anhydride groups and the oxygen groups of the silicates. The interlayer spacing of the clay mineral increases, and the interaction of the layers should be weakened. The clay mineral, intercalated with the oligomer of iPP-gMA, contacts sPP in the molten state during the processing. If the miscibility of the oligomers with sPP is good enough to disperse at the molecular level, a higher degree of intercalation and/or exfoliation of the intercalated clay mineral should take place. Although the bulk properties of sPP/clay nanocomposites were examined by Kaempfer et al. [16], there is no report to be found in the literature concerning the barrier performance of sPP/clay nanocomposite films. In this paper we report the structural characterization and the transport properties (sorption and diffusion of organic vapors) of sPP nanocomposites based on synthetic fluorohectorite modified by octadecyl ammonium ions (OLS), and maleic-anhydride-grafted isotactic polypropylene (iPP-g-MA) as compatibilizer. The aim was to investigate the effect of OLS content on the morphological organization which determines the mechanical and barrier properties.

2. Experimental

2.1. Materials

The synthetic clay used for our studies was fluorohectorite produced by CO-OP CHEMICAL Co., Japan, by heating together talcum and Na_2SiF_6. The trade name of this material is SOMASIF ME100 (ME). The cation exchange capacity (CEC) of ME is 0.7–0.8 meq/g. The interlayer spacing of the unmodified ME was 0.95 nm. The polypropylene (sPP) used for this studies was obtained from TOTALFINA, the trade name of the sPP is EOD 96-30, with a melt flow index (MFI) 4.4 g/10 min and a melting point of 130 °C. The maleic anhydride-modified PP oligomer was Hostaprime HC5 (MA content ~4.2 wt%; $T_m \sim 150$ °C; $M_n \sim 7500$ g/mol; $M_w/M_n \sim 3.9$ from Clariant GmbH, abbreviated as compatibilizer HC).

2.2. Preparation of organophilic layered silicates

Typically 1.20 mol of the octadecylamine and 1.20 mol HCl were dispersed in 20 l of 80 °C hot water. Then 1 kg of the fluorohectorite (Somasif ME100) was added to this mixture and stirred for 60 min. The precipitate was washed in a centrifuge with 150 l of deionised water. After the silicate had been dried at 80 °C for 48 h, it was ground in a mill (Retsch ZM100).

2.3. Compounding and preparation of polypropylene nanocomposites

sPP powder and the organophilic fluorohectorite were premixed in a tumbling mixer together with 0.25 wt% of stabilizer (Irganox1010/Irgafos168 Ciba: 4/1). This mixture was melt-blended together with the PP-g-MA in a corotating twin screw extruder (Collin; ZK 25T) at 190–230 °C and at 120 rpm. The obtained strands were pelletized and dried at 80 °C.

2.4. Film preparation

Films from the nanocomposites and the pure polymer were obtained by molding the pellets in a Carver Laboratory Press, and holding them at 180 °C for 10 min in order to destroy any memory of previous processing. The molded materials were rapidly quenched in an ice-water bath at a $T = 0$ °C and kept for 1 min. In the following, samples will be coded as sPPn, where n is the amount of OLS present in the nanocomposite. Pure sPP contains 20% iPP-g-MA.

2.5. Methods of investigation

Wide angle X-ray diffraction measurements (WAXS) were performed on the powder samples with a Philips diffractometer (equipped with a continuous scan attachment and a proportional counter) with Ni-filtered Cu Kα radiation.

The elastic moduli were derived from the initial part of the stress–strain curves, giving to the sample a deformation of 0.1%, (Dynamometric apparatus INSTRON 4301). The experiments were conducted at room temperature with the deformation rate of 2 mm/min. The initial length of the samples was 10 mm.

The transport properties were measured by the microgravimetric method, using a quartz spring balance having an extension of 1.62 cm/mg. The permeants were dichloromethane and *n*-pentane. The sorption was measured as a function of vapor activity $a = p/p_0$ where p is the actual

pressure (in mmHg) of the experiment, and p_0 the saturation pressure at 25 °C for dichloromethane (410 mmHg) and for *n*-pentane (510 mmHg).

Dynamic-mechanical properties were performed using a Polymer Laboratories Dynamic Mechanical Thermal Analyzer. The spectra were recorded in the tensile mode, obtaining the modulus E', and the loss factor, tan δ, at a frequency of 1 Hz, as a function of temperature. The heating rate was 5 °C/min in the range of −40–150 °C.

3. Results and discussion

3.1. Structure

In Fig. 1 the WAXD patterns of the sPP nanocomposites, in the range of $2\theta = 1–10°$, are reported. For comparison it is reported the diffractogram of the modified layered silicate, in which a diffraction peak at $2\theta = 4.17°$ appears. A basal spacing of 21.2 Å characterizes the original OLS. Generally the evidence of the intercalation or delamination of clay in the polymeric matrix is given by X-ray analysis. The peak of OLS is absent in samples sPP5 and sPP10, indicating clay exfoliation in these samples. For sample sPP20 it indicating a basal spacing of 33.0 Å in this sample. The melt-direct polymer intercalation of sPP into the OLS gives rise to nanocomposites in which the silicate layers were delaminated at low clay content, and ordered as in an intercalated structure in the sample with the highest clay content.

In Fig. 2 the X-ray diffractograms at higher values of 2θ reveal the obtained crystalline structure of sPP samples. We observe that all the samples crystallize in the disordered form I, having the chains in helical conformation, characterized by the main peaks at $2\theta = 12.3°$, 15.9° and 20.7°. Moreover this form becomes more and more disordered increasing the clay content. In fact, the peaks at 15.9° and 20.7° of 2θ are no longer distinguishable in sample sPP20. Therefore, the addition of clay does not change the usual crystalline form of sPP quenched at 0 °C, but increases the disorder. For comparison we report the spectra of the iPP-g-MA rapidly quenched at 0 °C. It shows the typical smectic form of iPP with low crystallinity represented by shoulders on the main 14.3° peak. It is worth noting that iPP-g-MA, present as 20% of the total amount for all the samples, is able to crystallize too. In fact, we observe the typical diffraction peak of iPP at 14.1° as a shoulder of the broad sPP diffraction peak at 15.9° and the diffraction peaks between 21.4° and 25.5° of 2θ.

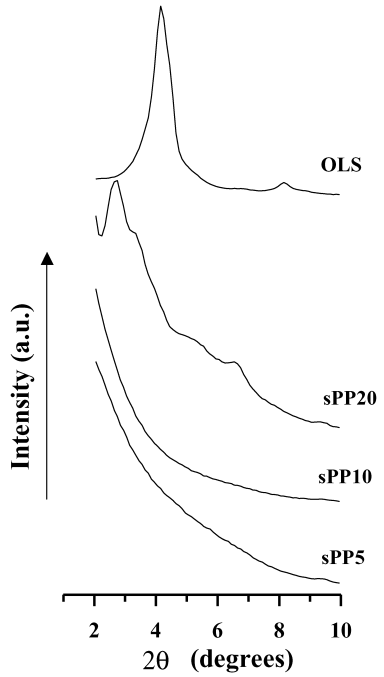

Fig. 1. Wide angle X-Ray diffraction patterns of the nanocomposites films and the OLS powders in the range of $2\theta = 1–10°$.

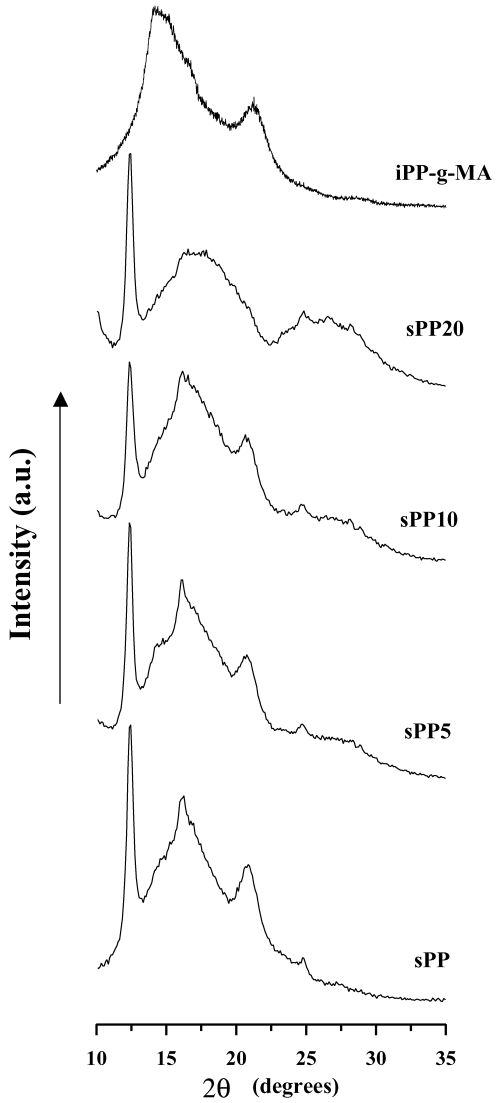

Fig. 2. Wide angle X-Ray diffraction patterns of the nanocomposites films, iPP-g-MA and pure sPP in the range of $2\theta = 10–35°$.

3.2. Mechanical properties

Generally, the nanometric dispersion of silicate layers in a polymeric matrix leads to improved modulus and strength, due to the stiffness of the silicate layers or even to possible layer or molecular orientation. The elastic modulus, E(MPa), as a function of the OLS content increases with increasing inorganic content (Fig. 3). This reinforcing effect seems to reach a plateau at clay contents higher than 20 wt%. It is interesting to note that the presence of 20% of iPP-g-MA increases the stiffness to 180 MPa already in the sample free of the inorganic component.

To investigate the stiffening effect in a broader temperature range we performed a dynamic-mechanical analysis. In Fig. 4(A) we show the dynamic storage modulus E', and in (B) the loss factor tan δ as a function of temperature, between -60 and 150 °C. The curves clearly show that the addition of clay into sPP increases the stiffness of all temperatures and even at high temperature, just before melting. At 100 °C the elastic modulus of the hybrid sPP sample with 20wt % of clay is three times higher than the value of the parent sPP sample. Correspondingly to the increase of the modulus the intensity of the tan δ values decreases. Location and form of the peak at about 20 °C corresponding to the glass transition temperature, is almost unchanged, although a less sharp dissipation peak, indicative of a broader distribution of Tg values, is observable for the hybrid materials.

3.3. Transport properties

The presence of the silicate layers may be expected to decrease the permeability due to a more tortuous path for the diffusing molecules that must bypass impenetrable platelets. The transport properties were measured with dichloromethane and *n*-pentane vapor. The use of two solvents of different molecular dimensions, solubility parameters, and different degree of interaction with the polymers, can give

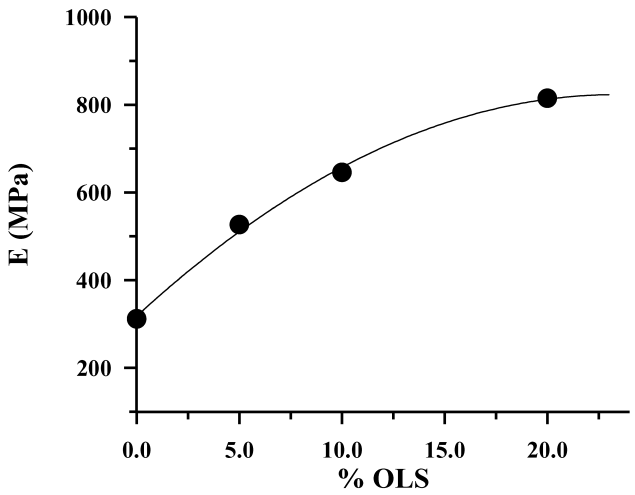

Fig. 3. Elastic modulus, E (MPa), as function of OLS percentage.

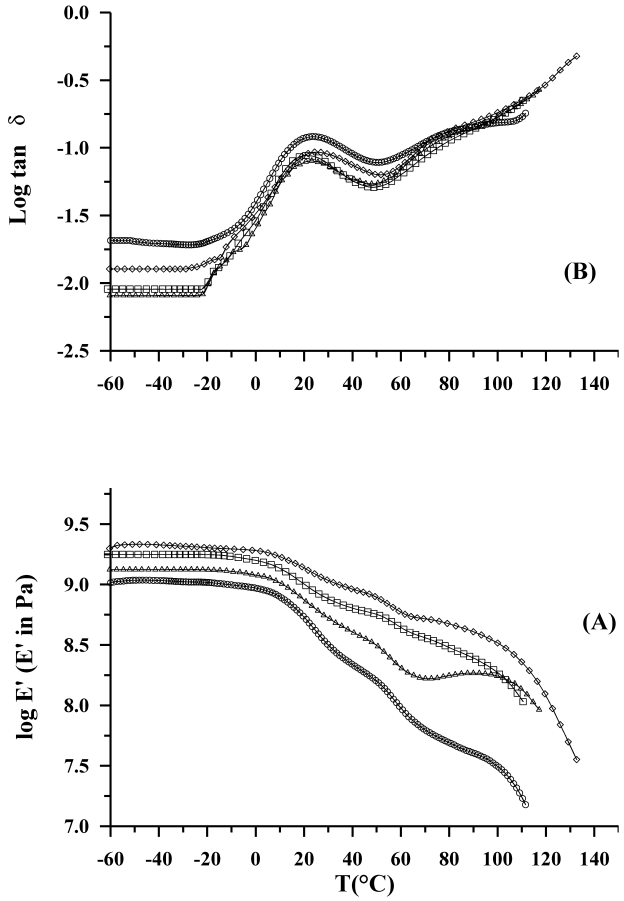

Fig. 4. (A) Log E' (E' in Pa) as function of temperature T (°C) and (B) Log tan δ as function of temperature T (°C) for: sPP (○), sPP5 (□), sPP10 (△) and sPP20 (◇).

useful information on the amorphous phases in the presence of both the crystalline phase and the impermeable OLS.

Measuring the increase of weight with time for the samples exposed to the vapor at a given partial pressure, gives the equilibrium value of the sorbed vapor, C_{eq}. Assuming Fickian behavior, the mean diffusion coefficient is derived from the linear part of the curve when C_t/C_{eq} is plotted vs square root of time [45–46]:

$$\frac{C_t}{C_{eq}} = \frac{4}{d}\left(\frac{D_t}{\pi}\right)^{1/2} \quad (1)$$

where C_t is the penetrant concentration at the time t, C_{eq} is the equilibrium value, and d is the thickness of the sample.

Diffusion in many polymer-solvent systems depends on concentration, and generally this dependence can be expressed by the following empirical law of Eq. (2) [47]:

$$D = D_0 \exp(\gamma C_{eq}) \quad (2)$$

where D_0 is the zero-concentration diffusion coefficient, related to the free volume and to the microstructure of the polymer; γ is a concentration coefficient, which depends on the free volume, and the plasticizing effectiveness of the penetrant.

The sorption parameter (S), is obtained from the equilibrium concentration (C_{eq}) of the permeant vapor as a function of the partial pressure (p) [48]:

$$S = d(C_{eq})/dp \quad (3)$$

The permeability of the samples is defined as [48–49]:

$$P = D_0 S \quad (4)$$

Although it has not a technological value, because it derives from the product of two ideal parameters, it is of fundamental importance in the purpose to correlate the physical properties and the structure of the samples.

3.3.1. Dichloromethane vapor

3.3.1.1. Sorption. The sorption curve (Fig. 5) follows the dual sorption-mode. The sorption isotherms show at low pressure values a linear dependence of sorption on activity, typical of a Henry sorption behavior, whereas an exponential increase on increasing vapor activity is observed at higher activities ($a > 0.3$), following a Flory–Huggins behavior [47]. Such isotherms represent the preference for the formation of penetrant–penetrant pairs, so that the solubility coefficient continuously increases with activity. The first molecules sorbed tend to locally loosen the polymer structure and promote sorption of the following molecules. These isotherms are observed when the penetrant effectively plasticizes the polymer, being a strong solvent or swelling agent for the polymer.

The numerical values of S (Eq. (3)) are reported in Table 1. The sorption coefficients of the nanocomposites are smaller compared to the pure sPP.

3.3.1.2. Diffusion. The diffusion for the samples sPP and sPP5 follows the Eq. (2) in the investigated concentration range (Fig. 6). The samples sPP10 and sPP20 show a linear decrease of the diffusion coefficient until about the 3% of solvent sorbed. The values of D_0, extrapolated in the low concentration range (ideal range), are reported in Table 1.

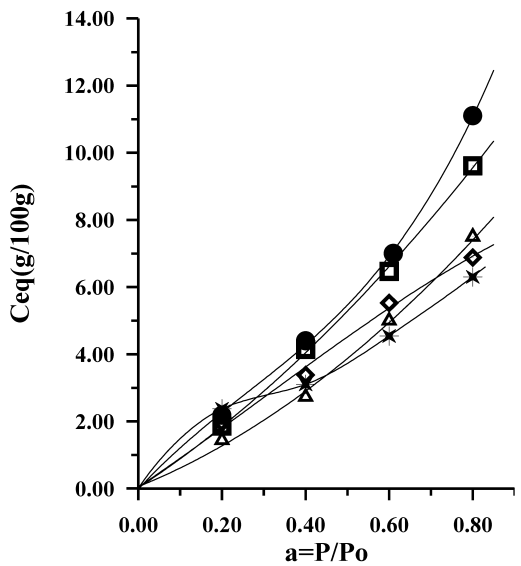

Fig. 5. The equilibrium concentration of dichloromethane, C_{eq} (g/100 g), as function of vapor activity, $a = P/P_0$, for: sPP (●), sPP5 (□), sPP10 (△), sPP20 (◇), OLS (∗).

Table 1
Transport properties of dichloromethane

Sample	S^a (g/100 g mmHg)	$D_0 \times 10^9$ (cm^2/s)
sPP	0.026	4.79
sPP5	0.024	1.07
sPP10	0.0175	0.213
sPP20	0.0220	0.187

[a] Evaluated according to Eq. (3).

The decrease of D_0 with increasing OLS content is attributed to a more tortuous diffusion path at low activity. At high activities, the vapor plasticizes the polymer, being a strong solvent or swelling agent for the polymer. The strong interaction with the penetrant molecules, leading to a high mobility of polymer chains, can induce structural transformations, as clustering of solvent molecules, crazing or partial dissolution. The system loose its compactness and diffusion becomes less dependent or even independent of concentration [48–51].

The permeability, P, of the nanocomposites was evaluated as the product of D_0 times S according to Eq. (4). The logarithm of P as a function of the OLS content linearly decreases until 10 wt% of the inorganic phase, and a plateau is reached from 10 to 20 wt% OLS (Fig. 7).

It is important to underline that this permeability is an ideal value, valid in a low vapor concentration range.

3.3.2. Pentane vapor

3.3.2.1. Sorption. The sorption isotherm of the organic modified clay mineral shows a typical Langmuir adsorption (Fig. 8). The solvent molecules are absorbed in specific

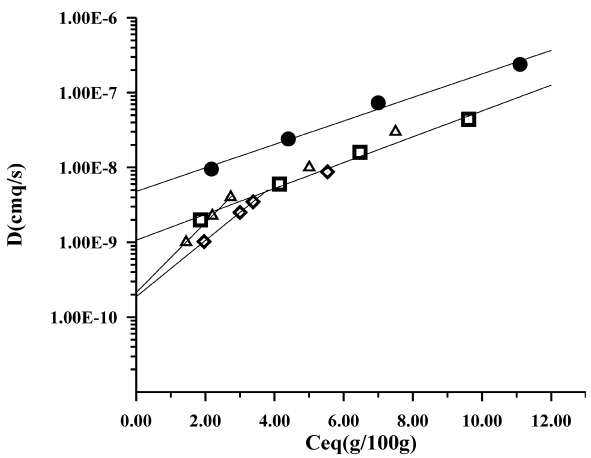

Fig. 6. The diffusion coefficient, D (cm^2/s), as function equilibrium concentration of dichloromethane sorbed, C_{eq} (g/100 g), for: sPP (●), sPP5 (□), sPP10 (△), sPP20 (◇).

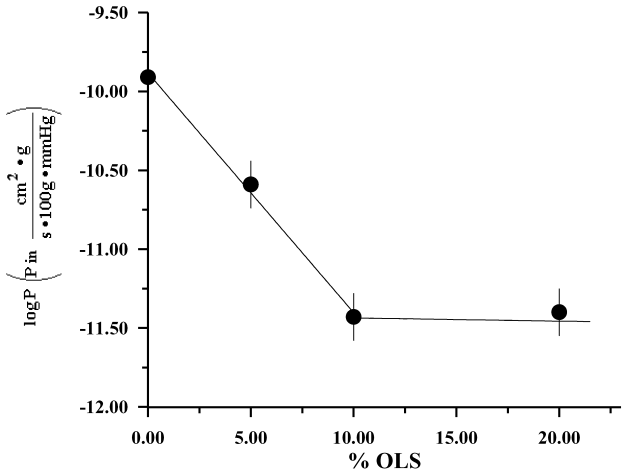

Fig. 7. The logarithm of permeability of dichloromethane as function of OLS percentage.

sites. When all the sites are occupied a constant value of concentration is shown on increasing the vapor activity [47]. The nanocomposites display a slight dual-sorption behavior, due to adsorption on specific sites of the clay mineral. The sorption was evaluated as reported for dichloromethane, at activity $a \leq 0.2$ (Table 2).

3.3.2.2. Diffusion. As in the case of dichloromethane, the differences of diffusion coefficients are evident at low values of solvent sorbed (Fig. 9 and Table 2). The permeability shows a significative decrease up to 5 wt% and a lower reduction in the range 5–20 wt% OLS (Fig. 10). Thus also for *n*-pentane vapor, the improvement of barrier properties, in terms of permeability, is mainly caused by the decreased diffusion.

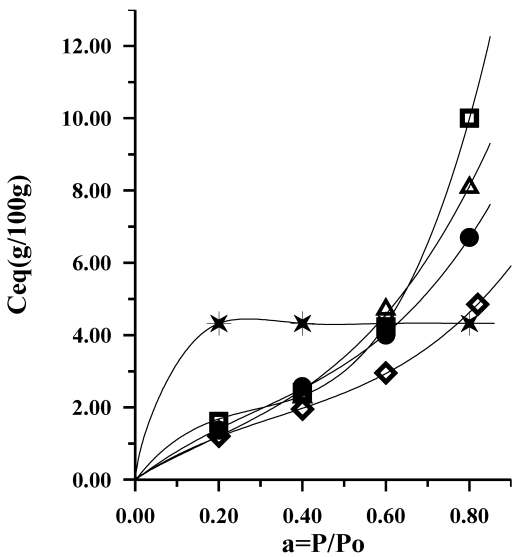

Fig. 8. The equilibrium concentration of *n*-pentane, C_{eq} (g/100 g), as function of vapor activity, $a = P/Po$, for: sPP (●), sPP5 (□), sPP10 (△), siPP20 (◇), OLS (∗).

Table 2
Transport properties of *n*-pentane

Sample	S[a] (g/100 g mmHg)	$D_0 \times 10^{11}$ (cm^2/s)
sPP	0.0470	3.59
sPP5	0.0160	1.90
sPP10	0.0130	1.67
sPP20	0.0117	0.754

[a] Evaluated according to Eq. (3).

4. Conclusions

The structural organization and the physical properties of sPP nanocomposites, obtained by melt blending organophilic layered silicates (OLS), sPP and iPP-g-MA as compatibilizer, were analyzed. X-ray analysis showed the delamination of the silicate at low clay percentages, and ordered intercalates at the highest clay content.

The elastic modulus of the samples was higher in a wide temperature range than of unfilled sPP, and increased with the inorganic content.

The sorption of dichloromethane and *n*-pentane was reduced compared to the unfilled sPP, but there were not significative differences between the samples having different clay concentration. The zero concentration diffusion coefficient D_0 also decreased with increasing clay content. The permeability for both vapors was reduced. In the case of dichloromethane, it showed a linear decrease until 10 wt% of the inorganic phase, and a plateau from 10 to 20 wt% of OLS. The permeability for *n*-pentane showed a significative reduction up to 5% then a linear decrease at 5–20 wt% of OLS. In both cases, the improvement of barrier properties, in terms of permeability, was largely caused by the reduced diffusion.

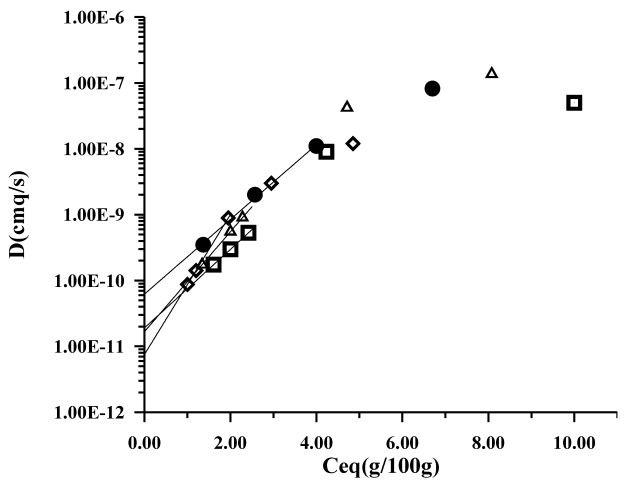

Fig. 9. The diffusion coefficient, D (cm^2/s), as function of equilibrium concentration of *n*-pentane sorbed, C_{eq} (g/100 g), for: sPP (●), sPP5 (□), sPP10 (△), sPP20 (◇).

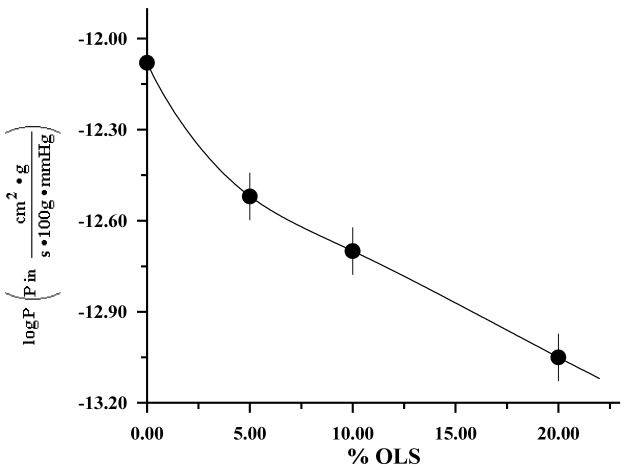

Fig. 10. The logarithm of permeability of *n*-pentane as function of OLS percentage.

Acknowledgements

The German authors thank the Sonderforschungsbereich SFB 428 of the Deutsche Forschungsgemeinschaft for the support of the nanocomposite research. The Italian authors thank the FISR Project, from the Italian Ministry of the University and Scientific Research, for the financial support.

References

[1] Komarneni SJ. J. Mater. Chem. 1992;2:1219.
[2] Giannelis EP. Adv. Mater. 1996;8:29.
[3] Ziolo RF, Giannelis EP, Weinstein BA, O'Horo MP, Granguly BN, Mehrota V, Russell MW, Hoffman DR. Science 1992;257:219.
[4] Alexandre M, Dubois P. Mater. Sci. Engng. 2000;28:1.
[5] Moet AS, Akelah A. Mater. Lett. 1993;18:97.
[6] Yano K, Usuki A, Okada A, Kurauchi T, Kamigaito O. J. Polym. Sci. A: Polym. Chem. Ed. 1993;31:2493.
[7] Shelden RA, Meier LP, Caseri WR, Suter UW, Hermann R, Muller M, Hegner M, Wagner P. Polymer 1994;35(8).
[8] Noh MW, Lee DC. Polym. Bull. 1999;42:619.
[9] Dietsche F, Mülhaupt R. Polym. Bull. 1999;43:395.
[10] Vaia RA, Giannelis EP. Polym. Commun. 2001;42:1281.
[11] Fisher HR, Gielgens LH, Koster TPM. Acta Polym. 1999;50:122.
[12] Liu L, Qi Z, Zhu X. J. Appl. Polym. Sci. 1999;71:1133.
[13] Reichert R, Nitz H, Klinke S, Brandsch R, Thormann R, Mülhaupt R. Macromol. Mater. Engng. 2000;275:8.
[14] Ma J, Qi Z, Hu Y. J. Appl. Polym. Sci. 2001;82:3611.
[15] Svoboda P, Zeng C, Wang H, Lee LJ, Tomasko DL. J. Appl. Polym. Sci. 2002;85:1562.
[16] Kaempfer D, Thomann R, Mülhaupt R. Polymer 2002;43:2909.
[17] Ewen JA, Jones JA, Razavi A, Ferrara JD. J. Am. Chem. Soc. 1988; 110:6255.
[18] Grisi F, Longo P, Zambelli A, Ewen JA. J. Mol. Cat. A: Chemical 1999;140:225.
[19] Uheara H, Yamazaki Y, Kanamoto T. Polymer 1996;37:57.
[20] Loos J, Buhk M, Petermann J, Zoumis K, Kaminsky W. Polymer 1996;37:387.
[21] Loos J, Petermann J, Waldofner A. Colloid Polym. Sci. 1997;275: 1088.
[22] Loos J, Schauwienold AM, Yan S, Petermann J, Kaminsky W. Polym. Bull. 1997;38:185.
[23] Guadagno L, Fontanella C, Vittoria V, Longo P. J. Polymer Sci. Polym. Phys. 1999;37:173.
[24] Loos J, Schimanski T. Polym. Engng. Sci. 2000;40:567.
[25] Bonnet M, Yan S, Petermann J, Zhang B, Yang D. J. Mater. Sci. 2001; 36:635.
[26] Guadagno L, D'Aniello C, Naddeo C, Vittoria V. Macromolecules 2000;33:6023.
[27] Men Y, Strobl G. Polymer 2002;43:2761.
[28] Guadagno L, D'Aniello C, Naddeo C, Vittoria V, Meille SV. Macromolecules 2002;35:3921.
[29] Lotz B, Lovinger AJ, Cais RE. Macromolecules 1988;21:2375.
[30] Lovinger AJ, Lotz B, Cais RE. Polymer 1990;31:2253.
[31] Lovinger AJ, Lotz B, Davis DD, Padden FJ. Macromolecules 1993; 26:3494.
[32] Chatani Y, Maruyama H, Noguchi K, Asanuma T, Shiomura T. J. Polymer. Sci. Part C 1990;28:393.
[33] Chatani Y, Maruyama H, Noguchi K, Asanuma T, Shiomura T. J. Polymer. Sci. Part B 1991;29:1649.
[34] De Rosa C, Corradini P. Macromolecules 1993;26:5711.
[35] De Rosa C, Auriemma F, Corradini P. Mackomol. Chem. 1996;29: 7452.
[36] De Rosa C, Auriemma F, Vinti V. Macromolecules 1998;31:7450.
[37] Lacks DJ. Macromolecules 1996;29:1849.
[38] Palmo K, Krimm S. Macromolecules 1996;29:8549.
[39] Ohira Y, Horii F, Nakaoki T. Macromolecules 2000;33:5566.
[40] Zhang J, Yang D, Thierry A, Wittmann JC, Lotz B. Macromolecules 2001;34:6261.
[41] Palmo K, Krimm S. Macromolecules 2002;35:394.
[42] Reichert R, Nitz H, Klinke S, Brandsch R, Thormann R, Muhlaupt R. Macromol. Mater. Engng. 2000;275:8.
[43] Ma J, Qi Z, Hu Y. J. Appl. Polym. Sci. 2001;82:3611.
[44] Svoboda P, Zeng C, Wang H, Lee LJ, Tomasko DL. J. Appl. Polym. Sci. 2002;85:1562.
[45] Bove L, D'Aniello C, Gorrasi G, Guadagno L, Vittoria V. J. Appl. Polym. Sci. 1996;62:1035.
[46] Barra G, D'Aniello C, Guadagno L, Vittoria V. J. Mater. Sci. 1999;34: 4601.
[47] Rogers CE. Physics and Chemistry of Organic Solid State. New York: Interscience Publisher; 1965.
[48] Gorrasi G, Tortora M, Vittoria V, Galli G, Chiellini E. J. Polym. Sci.: Part B: Polym. Phys. 2002;40:1118.
[49] Tortora M, Vittoria V, Galli G, Ritrovati S, Chiellini E. Macromol. Mater. Engng. 2002;287:243.
[50] Tortora M, Gorrasi G, Vittoria V, Galli G, Ritrovati S, Chiellini E. Polymer 2002;43:6147.
[51] G. Gorrasi, L. Tammaro, M. Tortora, V. Vittoria, D. Kaempfer, P. Reichert, R. Mülhaupt, J. Polymer Science Physics in press.